# Reconsidering electrophysiological markers of response inhibition in light of trigger failures in the stop-signal task

Skippen, P [1, 2]., Fulham, W. R [1, 2]., Michie, P.T [1, 2]., Matzke, D [3]., Heathcote, A [4]., Karayanidis, F [1,2,5].

Affiliations:

[1]*Functional Neuroimaging Laboratory, School of Psychology, University of Newcastle, Australia*

[2]*Priority Research Centre for Brain and Mental Health, University of Newcastle, Australia*

[3]*Psychological Methods, Department of Psychology, University of Amsterdam, The Netherlands*

[4]*Discipline of Psychology, School of Medicine, The University of Tasmania, Australia*

[5]*The Priority Research Centre for Stroke and Brain Injury, University of Newcastle, Australia*

Corresponding author:

Patrick Skippen

School of Psychology, University of Newcastle,

University Drive Callaghan NSW 2308, Australia

Phone: +61 2 4921 5076

Email: patrick.skippen@newcastle.edu.au

Keywords: *Stop-Signal Task, Response Inhibition, Trigger Failure, Attention, ERP, N1, N2, P3*

**Abstract**

Although advancements in electrophysiological methods to explore response inhibition have been substantial, the methods to describe behavioural differences in response inhibition have remained relatively unchanged. Here we use a model-based neuroscience approach to understand the neural correlates underpinning response inhibition as estimated using a recently developed ex-Gaussian hierarchical Bayesian model of stop-signal task performance. In a large healthy sample (N=156) of community drawn participants, we show the model-based estimates of stop-signal reaction time (SSRT) and a "trigger failure" parameter reflecting lapses of attention to task goals alter previously held interpretations of relationships between inhibition and event-related potential (ERP) component measures. Our results show clear attenuation of SSRT by ≈65ms when substantial levels of trigger failure are accounted for. This attenuation casts doubt on previous interpretations of the P3 as a manifestation of response inhibition. Instead, the N1, which reflects attentional processes, provides a better description of both SSRT and trigger failure than the P3. In particular, the peak N1 latency both correlated and coincided with ex-Gaussian estimated SSRT. Furthermore, participants with higher rates of trigger failure do not show a dissociation between N1 latency and the outcome of a stop trial. Our results show sufficient attentional control to elicit an inhibitory process is just as important, if not more so, than the speed of the process itself and that early ERPs provide a rich account of individual differences in both the speed and reliability of the inhibitory process.

## 1. Introduction

Response inhibition is a core component of cognitive control associated with the cancelation or suppression of an inappropriate behaviour (Bari & Robbins, 2013). It has been operationalised using paradigms such as the go/no-go (Falkenstein, Hoormann, & Hohnsbein, 1999) and the stop-signal task (SST; Logan & Cowan, 1984). In the SST, participants engage in a speeded choice response task. On a small proportion of randomly selected trials a stop signal occurs after the target stimulus, and participants must inhibit their response. The prominent horse-race model of the stop-signal task allows for what is usually assumed to be the main dependent variable of interest, stop-signal reaction time (SSRT), to be estimated. This model assumes that the construct of response inhibition is fully represented by the estimated latency of the 'stop process', a unitary process that is summarised by SSRT (Verbruggen & Logan, 2009).

It has been reported that SSRTs are slower in people with attention deficit hyperactivity disorder, schizophrenia, and substance use disorders, when compared to controls (for a review, see Lipszyc & Schachar, 2010). Increased SSRT is seen as representing less efficient response inhibition, resulting in reduced impulse control (but see, Sharma, Markon, & Clark, 2014; Skippen et al., 2019). However, the purity of SSRT as *the* measure of inhibitory cognitive control has recently been increasingly questioned (Band, Van Der Molen, & Logan, 2003; Logan, 1994; Matzke, Curley, Gong, & Heathcote, 2019; Matzke, Hughes, Badcock, Michie, & Heathcote, 2017; Matzke, Love, & Heathcote, 2016; Matzke, Love, & Heathcote, 2017; Skippen et al., 2019; Verbruggen, Best, Bowditch, Stevens, & McLaren, 2014; Verbruggen, McLaren, & Chambers, 2014).

### *1.1. Implications of Biased SSRT Estimations*

The horse-race model (Logan & Cowan, 1984) attributes the outcome of any given stop trial to a race between two independent processes: the go process that is measured by go RT and the stop process that is measured by SSRT. For example, if on a given trial, the go process finalises before the stop process, the response will not be inhibited (i.e., stop-failure trial). Alternatively, if the stop process finalises before the go process, the response will be successfully inhibited (i.e., stop-success trial). However, if either the go or the stop process fails to initiate on a given trial, the original horse-race model is not applicable. The model's inability to account for failures to engage the go or stop processes results in biased estimates of SSRT (Band et al., 2003; Matzke, Curley, et al., 2019; Skippen et al., 2019). While adjustments to traditional SSRT estimation methods have been developed to account for

omissions rates on go trials, as a close proxy for go failures (e.g., Tannock, Schachar, Carr, Chajczyk, & Logan, 1989), simulations suggest this method over-estimates SSRT (Verbruggen et al., 2019). Trigger failure (failure to initiate the stop process) has long been acknowledged as possible (e.g., Logan, 1994), yet it is not taken into account in non-parametric methods of estimating SSRT (see Verbruggen & Logan, 2009) and not accounting for trigger failure has been shown to bias estimates of SSRT in a growing number of studies (Band et al., 2003; Matzke, Curley, et al., 2019; Matzke, Hughes, et al., 2017; Matzke, Love, et al., 2017; Skippen et al., 2019). More generally, it is important to acknowledge that effective inhibitory control relies not only on fast SSRT, but also on the reliability of triggering the stop process (Chatham et al., 2012; Matzke, Love, et al., 2017).

We have previously described a parametric model of the SST in which the finishing times of the stop and go processes follow an ex-Gaussian distribution, and for which model parameters may be estimated with the Bayesian Estimation of ex-Gaussian Stop-Signal Reaction Time Distribution (BEESTS) procedure (Matzke, Dolan, Logan, Brown, & Wagenmakers, 2013; Matzke, Love, et al., 2013). This model has the distinct advantage of estimating the entire distribution of SSRT rather than only a summary measure obtained using traditional non-parametric methods (see Matzke, Verbruggen, & Logan, 2019, for an overview of the different estimation methods). The ex-Gaussian model used here (EXG3; Matzke, Curley, et al., 2019) extends that original model by incorporating failure to trigger a response to the go (go failure) and the stop (trigger failure; see also Matzke, Love, et al., 2013) stimulus, as well as accounting for go errors through separate racers corresponding to correct (matching) and error (mis-matching) responses to the go stimulus .

The practical importance of modelling trigger and go failures has been highlighted in a number of studies (Band et al., 2003; Matzke, Curley, et al., 2019; Matzke, Dolan, et al., 2013; Matzke, Hughes, et al., 2017; Skippen et al., 2019; Weigard, Heathcote, Matzke, & Huang-Pollock, 2019). For example, Skippen et al. (2019) found that the SSRT estimate derived from the EXG3 model was reduced by ≈100ms compared to the estimate obtained using the traditional non-parametric integration method (e.g., Tannock et al., 1989). Critically, this changed the relationships between SSRT and measures of impulsivity. When data were analysed with the non-parametric integration technique, impulsivity was correlated with estimated SSRT. However, application of the EXG3 model indicated that impulsivity was correlated with trigger and go failures rather than SSRT. Using a similar Ex-Gaussian model, Matzke, Hughes, et al. (2017) found both higher levels of trigger failure and

slower SSRT in patients with schizophrenia when compared to controls[1]. The distribution of SSRT suggested that the delay in the stop process was largely due to poor encoding of the stop signal, rather than a slower inhibition process per se. They argued that the increased probability of trigger failure and the delayed initiation of the stop process could be attributable to deficits in attention. Therefore, attentional factors may play a larger role in inhibitory ability than previously thought. In this study, we take a model-based neuroscience approach to better understand the stopping process and trigger failure (Sebastian, Forstmann, & Matzke, 2018), using electroencephalogram (EEG) activity recorded during the SST to capture the timeline of cognitive processes involved in stop-success and stop-failure trials.

### *1.2. Temporal processes of response inhibition*

Event Related Potential (ERP) components time-locked to an auditory stop signal typically consist of an early negative component (N1) within the first 100-200ms, a negative deflection (N2) occurring around 200ms, and a positive component (P3) around 300-350ms, all commonly measured fronto-centrally (Pires, Leitão, Guerrini, & Simões, 2014). These components are thought to index distinct processes that together result in the inhibition of a pre-potent response.

The N1 is thought to reflect the level of encoding of a stimulus within the auditory cortex (Hillyard, Hink, Schwent, & Picton, 1971; Luck, Woodman, & Vogel, 2000; Näätänen & Picton, 1987). The N1 is comprised of several underlying components that are influenced by voluntary attention to the stimulus, the physical attributes of the stimulus, and the conditions under which it is presented (Näätänen, 1982; Näätänen, Gaillard, & Mäntysalo, 1978; Näätänen & Michie, 1979; Näätänen & Picton, 1987). In the response inhibition literature, N1 is commonly used as a measure of attentional resources allocated to the stop signal (Bekker, Kenemans, Hoeksma, Talsma, & Verbaten, 2005; Dimoska & Johnstone, 2008). The commonly reported 'stop-N1' effect (i.e., increased N1 amplitude for stop-success compared to stop-failure trials), suggests that N1 amplitude is associated with the outcome of the stop process (Bekker et al., 2005; Hughes, Fulham, Johnston, & Michie, 2012; Lansbergen, Böcker, Bekker, & Kenemans, 2007). This 'stop-N1' effect has been suggested to reflect a mechanism that primes the detection of the stop signal, in turn potentiating a faster

[1] This study used the BEESTS procedure with trigger failure, and therefore did not estimate go failure.

connection between brain regions vital to improving the speed of inhibition (Kenemans, 2015).

The role of the two later components, N2 and P3, is the subject of substantial debate. It is generally thought that N2 reflects conflict monitoring and cognitive control, whereas P3 represents the inhibition process (for a review, Huster, Enriquez-Geppert, Lavallee, Falkenstein, & Herrmann, 2013). These attributions arise largely from the relative timing of the two components relative to SSRT. Supporting the argument that the P3 represents the inhibition process, the onset latency of the P3 has been found to coincide with SSRT latency (Kok, Ramautar, De Ruiter, Band, & Ridderinkhof, 2004; Wessel & Aron, 2015). Alternatively, others have argued that P3 peaks too late to represent inhibition, and instead is more likely to reflect post-inhibitory processing (González-Villar, Bonilla, & Carrillo-de-la-Peña, 2016; Huster et al., 2013; Ramautar, Kok, & Ridderinkhof, 2004). However, both arguments are based on conventional estimates of SSRT, which as discussed above, are likely biased because they do not account for trigger and/or go failure. As models that account for trigger failure produce attenuated estimates of SSRT, the temporal association between ERPs (especially P3) and SSRT are likely to be altered. For example, estimates of SSRT derived from the EXG3 model that accounts for trigger and go failures (Skippen et al., 2019) align the end of the stop process within the latency range of N1 and N2 components, that is, at least 100ms before the onset of the P3. Therefore, models that include these failure parameters in the estimation of SSRT may challenge previous interpretations of the ERP correlates of response inhibition.

The only previous study to investigate the relationship between ERPs and parameters from an ex-Gaussian model of the SST reported that faster stop-N1 latency was associated with higher probability of trigger failure in a small group of people with schizophrenia (Matzke, Hughes, et al., 2017). At face value, this relationship is counterintuitive, suggesting that earlier processing of the stop signal (as indexed by the N1) is predictive of higher rates of trigger failure. However, as the N1 is comprised of a number of partially overlapping sub-components (Näätänen & Picton, 1987), Matzke, Hughes, et al. (2017) argued that earlier N1 peak latency may arise from attenuation of a late N1 sub-component and not necessarily represent faster processing of the stop signal. This would be consistent with the hypothesis that trigger failure results from dysfunctional encoding of the attributes of the stop signal, which then fails to generate the appropriate response pattern (i.e., inhibition). However, the Matzke, Hughes, et al. (2017) analysis was based on a relatively small group ($N \leq 13$ for

patients and controls), and did not separately examine stop-successes and failures, so these findings need replication before drawing strong conclusions about the relationship between ERP components and model parameters.

### *1.3. Current study*

In the present study, we examine the relationships between EXG3 parameters and ERPs to the stop signal in a large, young, healthy cohort (*N* = 156). With increased statistical power and opportunity to examine individual variability, we aim to provide insight into the neural processes that underlie trigger failure, go failure, and SSRT. We expect to replicate the finding that trigger failure rate is negatively associated with stop signal N1 peak latency. We will also estimate the onset latency of the N1 component to examine whether trigger failure is associated with early or late N1 sub-components. Furthermore, we will examine whether ERP components for successful and failed stop trials correlate with the same model parameters. In line with the attentional account of trigger failure, we expect that lower levels of attention to the stop signal (i.e., reduced N1 amplitude) will be related to higher rates of trigger failure.

As SSRT latency is attenuated after accounting for trigger failure, we expect that the relationships between SSRT and ERP components commonly reported in the literature will be altered. Specifically, we expect to challenge the common interpretation of the P3 as an index of response inhibition process by showing that, after accounting for trigger failure, the commonly reported positive relationship between SSRT and P3 will be reduced. We will test the relationships between P3 onset and peak latency, and peak amplitude with both traditional and EXG3 estimations of SSRT. As theorists have recently suggested that response inhibition is a more automatic process than previously thought (Verbruggen, McLaren, & Chambers, 2014), we expect EXG3 estimated SSRT will have a stronger relationship with early ERP components (i.e., N1, N2) than the traditional estimation. Finally, we will run exploratory analyses of the relationships between the remaining model parameters and ERP component measures to inform future hypotheses about the neural correlates of response inhibition in a large healthy young sample. These include the relationships between the N2 and all EXG3 parameters, and the relationships for both the N1 and P3 with go RT and go failures.

## 2. Methods

### *2.1. Participants and Procedure*

The data reported here were collected as part of a larger longitudinal study, the Age-ility Project (Karayanidis et al., 2016). Participants were screened for self-reported neurological or psychiatric conditions and asked to abstain from caffeine or alcohol for 2hrs prior to testing. A community-based cohort aged 15-35 years (*n*=282) was recruited via local businesses, community groups, and secondary and tertiary education centres. Participants were paid AU$20/hr. This study conforms to the Declaration of Helsinki and was approved by the University of Newcastle Human Research Ethics Committee (HREC: H-2012-0157).

Participants attended the laboratory on two occasions. In the first session, they completed a neuropsychological battery and received demographic and psychometric questionnaires to complete at home. In the second session, participants initially practiced and then performed a task switching paradigm (see Cooper et al., 2015) with concurrent EEG recording for approximately 45 minutes before completing the SST. After loss to attrition between testing sessions, 208 participants attempted the stop-signal task. EEG technical problems resulted in the removal of 20 participants. Model constraints excluded a further 32 participants. The final total sample was N = 156 (see *2.3.1. Data Cleaning*). This sample overlaps with that reported by Skippen et al. (2019), with the exclusion of participants without clean EEG.

### *2.2. Stimuli and Apparatus*

*2.2.1. Stop-signal task.* The primary go task was a two-choice number parity task (700 trials). The stimulus was a number between 2 and 9, presented for 100ms in the centre of a grey rectangle. On 29% of trials (≈200 trials), the go stimulus was followed after a variable stop-signal delay by an auditory stop signal delivered binaurally through calibrated headphones (1000Hz, 85dB tone, 100ms duration). The stop-signal delay ranged from 50-800ms and decreased or increased by 50ms after every failed or successful stop trial, respectively. Following a single practice block, behavioural responses and EEG activity were recorded for 700 trials across five blocks.

*2.2.2. Electroencephalogram recording.* EEG data were recorded (2048Hz sample rate, bandpass filter of DC-400Hz) via a BioSemi Active Two system with 64 scalp electrodes as well as two mastoid, lateral ocular, and infra/supra ocular sites. Common mode sense and driven right leg electrodes were positioned inferior to P1 and P2, respectively. Data were

recorded relative to an amplifier reference voltage and re-referenced to the common average offline to remove common-mode signals.

### *2.3. Data analysis*

*2.3.1. Data Cleaning.* At the start of the study, a technical issue resulted in the first 20 participants being excluded. Another 32 participants were excluded from analysis due to poor or non-compliant performance on the stop-signal task. Of these, (a) nine participants slowed their go trial reaction time by over 300ms over the course of the experiment[2], most likely to assist in inhibiting on a subsequent stop trial. This slowing of responses can bias SSRT estimates; (b) four participants responded on over 75% of stop trials, against what would be expect of the stop-signal delay algorithm; (c) sixteen were excluded because they violated the independence assumption of the horse race model. This assumption states that the go and stop processes are independent and is tested by confirming that mean RT on stop trials (i.e., stop-failure trials) is not slower than mean RT on the go task; (d) one participant had both independence and response rate violations; (e) one had both independence violations and commission error rates on go task approaching chance, and (f) one participant had zero errors on the go task and therefore could not be modelled with the EXG3. This resulted in an exclusion rate of approximately 16.5% (not including the hardware error).

During the quality control process, we found six participants with a block of behavioural data that differed from the rest of their performance. One participant made no responses with their right hand across the entire 5th block, and one reported forgetting to stop to the signal in the first block but corrected this for the remaining blocks. Three participants made no responses at all in one block (1st, 2nd, or, 4$^{th}$, respectively), and the final participant made no successful stops in the first block. For each participant, these block with the problem performance was removed from further analysis. In all cases the SSD tracking recovered quickly in the following block of trials.

*2.3.2. Modelling of Response Inhibition.* The ex-Gaussian distribution is a convolution of a Gaussian (i.e., normal) and an exponential distribution. The EXG3 model (Heathcote et al., 2018) assumes that finishing times of the three runners (i.e., two go runners and one stop runner) can be described by an ex-Gaussian distribution. The model estimates the finishing time of both the matching (correct) and mis-matching (error) response to the go stimuli. For each of the go processes (matching and mis-matching) and the stop process, the ex-Gaussian

[2] This was assessed by regressing RT on trial number and then using the slope of the fit to estimate slowing over the course of the task.

distribution has three parameters μ, σ, and τ, which characterise the mean and standard deviation of the normal component, and the mean of the exponential component (i.e., the long slow tail of the distribution), respectively. The mean and variance of each parameter can then be estimated as $\mu + \tau$ and $\sigma^2 + \tau^2$, respectively. The parameters quantifying the probability of go and trigger failures were estimated on the probit scale.

We used the Dynamic Models of Choice (DMC; Heathcote et al., 2018) software implemented in R (R Core Team, 2018) to estimate model parameters via Bayesian hierarchical modelling. In hierarchical modelling, the population-level mean and standard deviation parameters characterise the population-level distribution for each model parameter. Weakly informative uniform priors were set for the population-level parameters, which are identical to those of Skippen et al. (2019). Posterior distributions of the parameters were obtained using Differential Evolution Markov Chain Monte Carlo (MCMC) sampling (Ter Braak, 2006), with steps closely mimicking Heathcote et al. (2018).

To confirm the non-negligible presence of trigger failures, we ran two EXG3 models, one with a trigger failure parameter and one without. We ran 33 MCMC chains in the model with trigger failure and 30 in the model without (e.g., three times as many chains as model parameters). Participants were initially modelled separately until the MCMC chains reached convergence, with thinning of every $10^{th}$ sample. Convergence was identified with visual inspection and Gelman-Rubin $\hat{R}$ (Gelman & Rubin, 1992) values below 1.1. These participant fits were then used as the start values for the hierarchical fits. During this period, we set a 5% probability of migration for both the participant and the hierarchical levels. Crossover steps were performed until chains were converged and stable. After this, an additional 200 samples per chain were retained as the final set from which further analysis is undertaken.

The population distributions describe the between-subject variability of the parameters and are appropriate for population inference, analogous to frequentist random-effects analysis. On the other hand, the individual participant parameters are useful for examining individual differences and are used here to examine the relationships between response inhibition and electrophysiology.

*2.3.3. Electrophysiological Data.* EEG data pre-processing was performed using in house techniques within EEGDisplay v6.4.4 (Fulham, 2015). The continuous EEG records were firstly down sampled to 512Hz before being visually inspected to exclude intervals containing gross artefact. Bad EEG channels were replaced by interpolating between adjacent scalp electrodes. Eye blink artefact was corrected using a regression-based procedure (Semlitsch,

Anderer, Schuster, & Presslich, 1986). As a secondary control measure to visual inspection, gross movement or muscle artefacts were excluded with an automated procedure which applies amplitude thresholds within specific frequency bands. For each electrode a threshold of 4, 6, and 7.5 times the standard deviation in the EEG signal was set for the frequency bands below 2Hz, between 0.5-15Hz, and above 10Hz, respectively. EEG was then bandpass filtered between 0.05 and 30Hz and re-referenced to the average of the left and right mastoids.

EEG epochs were extracted between 900ms pre-event to 1400ms post-event for the stop signals and averaged to obtain stop-locked ERPs separately for stop-success and stop-failure trials. Stop-locked ERPs are contaminated by the overlapping perceptual response to the preceding go stimulus, especially for short stop-signal delays. Assuming the underlying responses elicited by the go stimulus and by the stop signal combine linearly, we extracted the underlying stop-locked ERPs by applying level 1 ADJAR correction (Woldorff, 1993), which takes into account the observed distribution of stop-signal delays between the go stimulus and the stop signal. The ADJAR corrected stop-locked ERPs were baseline corrected to the 50ms peri-stop (i.e., -25 pre- to 25ms post-stop).

The extracted amplitude and latency measures for ERP components were calculated using the *geterpvalues* function from the ERPLAB (Lopez-Calderon & Luck, 2014) package for MATLAB (Mathworks, r2018b). To increase the resolution of latency estimates, we first interpolated waveforms by a factor of four to a 2048Hz sampling rate. Peak latency was estimated using fractional area latency, the latency that defines 50% of the area under the curve across a specified window after stop-signal onset (N1 = 80 – 185ms; P3 = 290 – 400ms). Fractional area latency is less sensitive to noise than simple peak latency (Kiesel, Miller, Jolicœur, & Brisson, 2008). For N1 and P3 peak amplitude, we took an average of 20ms around the respective peak latency values. The onset latency of N1 was estimated by determining the latency at which the amplitude reached 50% of the component's peak amplitude. The relatively flat morphology of the P3 meant that, for some participants, the estimation of this component was difficult and therefore we used 60% of the peak amplitude to obtain more robust onset latency estimates. As the N2 component did not show a distinct peak in average ERPs for the majority of participants, we extracted mean amplitude over 190 – 245ms.

As per the literature, we expected midline, frontal/fronto-central sites to show the largest effects for these components. We extracted component measures from midline sites

(Fz, FCz, Cz, CPz, Pz), and corresponding lateral sites (F3, F4, FC3, FC4, etc.). Figures showing ERPs display 95% confidence intervals appropriate for within-subject comparisons calculated through the adjusted Cousineau-Morey method (Morey, 2008). These figures were used in determining the site/s of interest.

*2.3.4. Plausible Values Analysis.* Traditional tests of correlations between model parameters and ERP component measures ignore the uncertainty of the parameter estimates, and so tend to be overconfident. Here we use a plausible value analysis to evaluate these relationships, which calculates a distribution of correlations between covariates (e.g., N1 latency) and model parameters (i.e., mean SSRT) using each MCMC sample from the posterior distribution of the parameter. Ly et al. (2018) provide a detailed rationale for this fully Bayesian and more conservative approach, which is more appropriate for the novel effects examined here. This process results in a set of 'plausible' values of the sample correlation, *r*, for n individuals. As described by Ly et al., the sample correlation can be transformed into the posterior distribution of the population correlation (rho; ρ), which is a function of *r* and *n*. Repeating this process for all plausible sample correlations and averaging each population correlation distribution yields the estimated posterior distribution of the population correlation.

**2.4. Statistical Procedures**

*2.4.1. Stop-Signal Task Behaviour.* In accordance with the recommendations of Matzke, Verbruggen, and Logan (2019), we describe the mean RT on both correct go and stop-failure trials to test the independence assumption of the horse-race model. Omission and commission error rates on the go task are reported, along with the mean and range of stop-signal delays. We report the mean and standard deviation of the traditional SSRT estimate, $SSRT_{int}$, obtained using the integration technique described in Verbruggen et al. (2019), where go omissions trials are replaced with the participants maximum go RT.

*2.4.2. Model Selection and Parameter Estimation.* To determine the effect of incorporating the trigger failure parameter, we estimated two EXG3 models, one with a trigger failure parameter and one without. Both models included a go failure parameter, as Matzke, Curley, et al. (2019) demonstrated that this parameter may be included in the model without causing estimation problems even if go omissions are infrequent. To formally compare the two hierarchical models and examine whether the presence of trigger failures was non-negligible, we used the Deviance Information Criterion (DIC; Spiegelhalter, Best, Carlin, & Van Der Linde, 2002). Smaller DIC values indicate a better model in terms of providing an

accurate yet parsimonious fit to the data. When comparing models, a difference in DIC of 10 or more is taken as substantial evidence in favour of the model with the smaller DIC. Furthermore, we assessed the absolute goodness-of-fit using posterior predictive model checks. The process of posterior predictive checks involves randomly selecting a set of, in this case 100, parameter vectors from the joint posterior of the participant-level model parameters. Following this, 100 stop-signal data sets are generated using the parameter vectors. If the model provides an adequate representation of the data, these predictions should closely resemble the observed data[3]. We used the most supported EXG3 model to estimate mean SSRT (i.e., $\mu_{stop} + \tau_{stop}$), mean finishing time of the matching go runner (i.e., $\mu_{go\ correct} + \tau_{go\ correct}$), go failures, and trigger failures. We refer to the EXG3-based estimate of mean SSRT as $SSRT_{EXG3}$.

*2.4.3. ERP Component Electrode Site/s of Interest.* To determine the site/s of interest for each ERP component measure, we examined the scalp topography of the grand average ERP component windows and compared these with previous literature. Furthermore, we used a Bayesian paired t-test to determine the site/s with the largest amplitude differences between trial types (i.e., stop-failure vs stop-success) for each ERP component measure. Two-sided Bayesian t-tests were computed using the *BayesFactor* package (Morey & Rouder, 2018) in R (R Core Team, 2018), with effect sizes given as the posterior median effect size (δ). Priors for the t-test on trial type were default "medium" Cauchy priors with $r = \sqrt{2}/2$.

*2.4.4. Traditional Correlational Analysis.* Correlations between $SSRT_{int}$ and ERP component measures were undertaken using Pearson product moment correlations. Inference was conducted using Bayes factors. Correlation tests were completed with a prior on ρ centred around zero, assigning equal likelihood for all values between -1 and 1. A default "medium" *r* scale arguments of $1/3$ were used. We use the Kass and Raftery (1995) conventions to describe the strength of evidence that the data provide for the alternative hypothesis. For the null and alternative, a Bayes factor between 1/3 and 3 is considered 'equivocal' (i.e., indicating more data are needed to obtain a clear outcome), between 1/3-1/20 or 3-20 is

[3] We report a small but systematic tendency for the inhibition function predicted by the EXG3 model to be steeper than the observed inhibition function (see also, Skippen et al., 2019). This effect was most prominent in participants with less stable RT (i.e., speeding or slowing across the task). Therefore, we ran two further hierarchical models containing the 50 and 100 most stable participants. Details of these analyses are found online at osf.io/rhktj. Most importantly for this study, fits to inhibitions functions were greatly improved in these models, and inferences based on the plausible values analysis was consistent across all models.

considered 'positive', between 1/20-1/150 or 20-150 'strong', and Bayes factors less than 1/150 or greater than 150 are considered 'very strong'.

*2.4.5. Plausible Values Analysis.* To first examine the overlap between traditional and model estimates of response inhibition on the stop-signal task, we examined the relationship between the posterior distributions of the mean $SSRT_{EXG3}$, probit transformed trigger and go failure parameters and $SSRT_{int}$ using plausible values analysis. We also report plausible value correlations between model parameters and ERP component measures from both stop-success and stop-failure trials. All plausible values relationships are accompanied by associated Bayesian *p*-values, which denote the proportion of the distribution shifted away from zero. For example, a Bayesian *p* value of .05 denotes that 95% of the resulting distribution is above (for positive relationships) or below (for negative relationships) zero. In acknowledgement of the large number of plausible values tests, we take a Bayesian *p* value <.01 as reliable. This method also allows for the comparisons of two sets of plausible values relationships. For each relationship we can take differences between samples from each plausible value distribution and if the resulting difference distribution returns a Bayesian *p* value <.01, we have evidence so say that the difference in relationships is reliably greater than zero. This method was used to test whether relationships between $SSRT_{EXG3}$ and the N1 are stronger than between $SSRT_{EXG3}$ and P3. Code for this analysis can be found in the materials at osf.io/rhktj (*made public at acceptance*).

## 3. Results

### *3.1. Stop-Signal Task Behavioural Summary*

Of the 198 ± .85 stop trials (mean ± SEM), participants responded on average to 49.14% ± .45% of stop trials, showing the efficacy of the tracking algorithm. Of the 479 ± 2.7 go trials, errors of omission and commission occurred on 2.99 ± .31 % and 7.41 ± 0.51% of trials, respectively. The mean stop-signal delay was 354.24 ± 9.63ms (range = 89.42 – 705.29ms). Mean RT on correct go trials was 585.56 ± 7.37ms. Mean RT on stop-failure trials was 521.69 ± 6.09ms, faster than the average go RT. The slope of a regression of RT against trial number indicated that participants slowed their responses by an average of only 43.58 ± 7.63ms between the start and end of the test session. Lastly, traditional estimation via the integration technique returned a mean $SSRT_{int}$ of 196.91 o± 7.43ms.

### *3.2. Model Selection and Parameter Estimation*

Both models achieved convergence, as determined by visual inspection and a Gelman-Rubin $\hat{R}$ <1.1. The fit generated from the EXG3 model with trigger failure was more

closely matched to the observed data than the model without trigger failure (DIC difference = 1685). Hence, we selected the EXG3 model with trigger failure for use in all further analyses. A visualisation of the posterior distributions of the parameter estimates from the EXG3 model that included trigger failure is presented in Figure 1. The EXG3-based estimate of mean $SSRT_{EXG3}$ has a mean of 132.35ms with a 95% credible interval of [124.55, 140.17], which was around 65ms faster than $SSRT_{int}$. Trigger failure rates were 22.27% [21.43, 24.82], suggesting that across participants, an average of 22% of stop-failure trials were due to a failure to trigger an inhibitory response. Go failures occurred on 3.06% [2.83, 3.76] of trials. Lastly, the mean finishing time of the matching go runner was 596.51ms [581.13, 611.84].

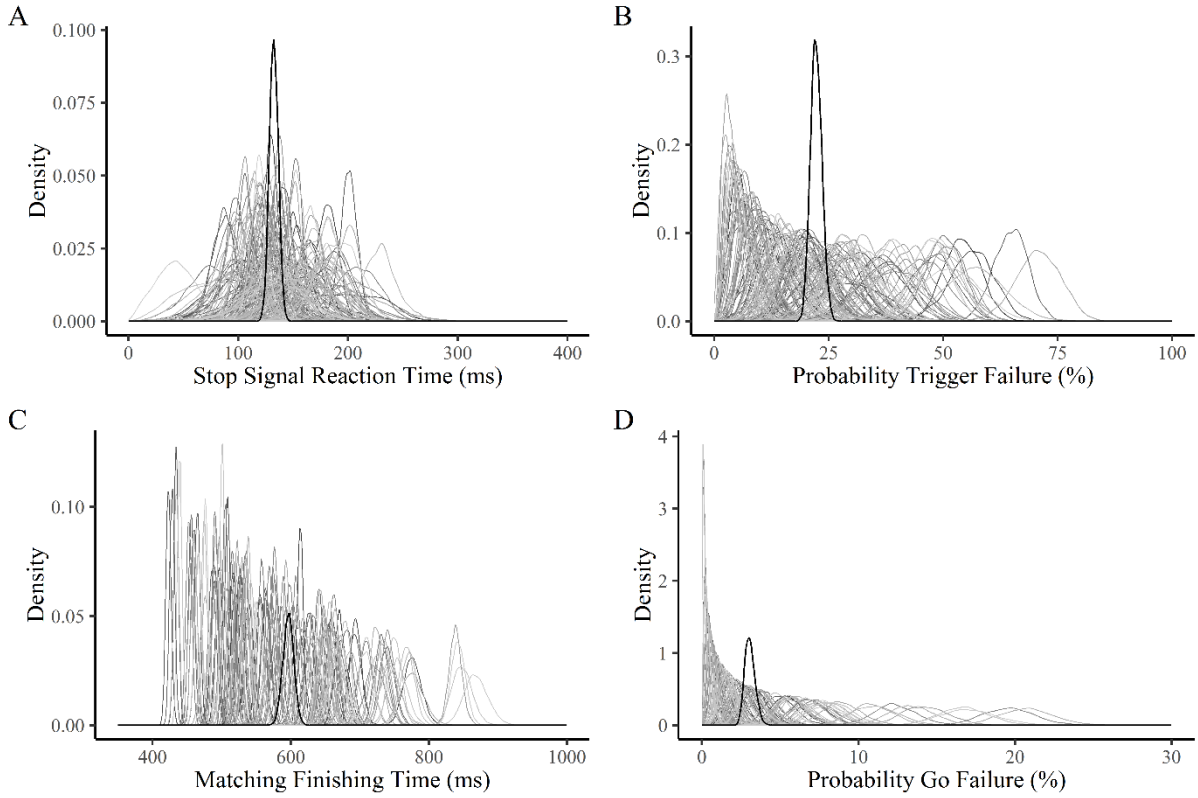


***Figure 1. Posterior distributions of the individual (gray density lines) and group-level mean (black boldface density lines) parameters. Mean Stop Signal Reaction Time (Milliseconds; Panel A). Probability of Trigger Failure (Panel B). Mean finishing time for the matching go runner (Milliseconds; Panel C). Probability of Go Failure (Panel D). Each grey shaded distribution represents the posterior of a single participant. The black boldface distribution represents the posterior distribution of the population-level mean parameter.***

### *3.3. ERP Summary*

The summary statistics of ERP components are found in Table 1. Based on previous literature, as well as the morphology and topography of ERP waveforms, and the strength of trial-type differences, we selected FCz for measurement of the N1 and N2 component

(Figure 2). The N1 was larger, peaked earlier, and had an earlier onset on stop-success, compared to stop-failure trials (Table 1). However, the evidence for a trial type difference and the effect size was much larger for peak latency ($BF_{10}$ = $5.25e^{13}$, δ = -.77) than amplitude ($BF_{10}$ = 10.59, δ = -.14). The N2 was generally under the baseline (Figure 2), but stop-failure trials had larger (i.e., less positive) N2 amplitude than stop-success trials (Table 1, $BF_{10}$ = $2.7e^{17}$, δ = .9).

**Table 1. Summary statistics for and differences between trial types for each component measure at FCz.**

| | Measure | Stop Success (SD) | Stop Failure (SD) | Trial Difference ($BF_{10}$) | Effect Size (δ) |
|---|---|---|---|---|---|
| **N1** | | | | | |
| | Latency (ms) | 127.86 (8.97) | 133.22 (10.81) | $5.25e^{13}$ | -.77 |
| | Amp (μV) | -13.50 (5.99) | -12.67 (6.04) | 10.589 | -.14 |
| | Onset (ms) | 93.39 (11.71) | 96.64 (14.16) | 188.985 | -.29 |
| **N2** | | | | | |
| | Amp (μV) | 4.64 (5.89) | 1.00 (5.01) | $2.66e^{17}$ | .9 |
| **P3** | | | | | |
| | Latency (ms) | 313.56 (23.22) | 312.60 (27.14) | .093 | -.30 |
| | Amp (μV) | 7.28 (4.29) | 6.03 (4.00) | $2.38e^{5}$ | .74 |
| | Onset (ms) | 291.04 (29.19) | 291.43 (34.07) | .758 | -.44 |

*Note.* Effect sizes are for the success – failure trial type difference. Shading indicates at least weak evidence in favour of the trial type difference. Cross-hatching indicates at least weak evidence in favour of a null difference.

Figure 2 shows that the P3 component spread anteriorly from Pz to FCz. Interestingly, while trial type effects were equally large at FCz and Pz, the peak latency difference between these sites suggests a P3a/P3b dissociation (Figure 2). As we focus on the inhibition-related P3, we measured it at FCz to be consistent with prior literature (results of analysis at Pz can be found in the supplementary materials). There was very strong support for a trial type difference in P3 amplitude ($BF_{10}$ = $2.38e^{5}$, δ = .74), showing that stop success trials had a larger amplitude. Howevr, there was equivocal support for a difference in onset latency, and positive support for a null difference in peak latency (Table 1).

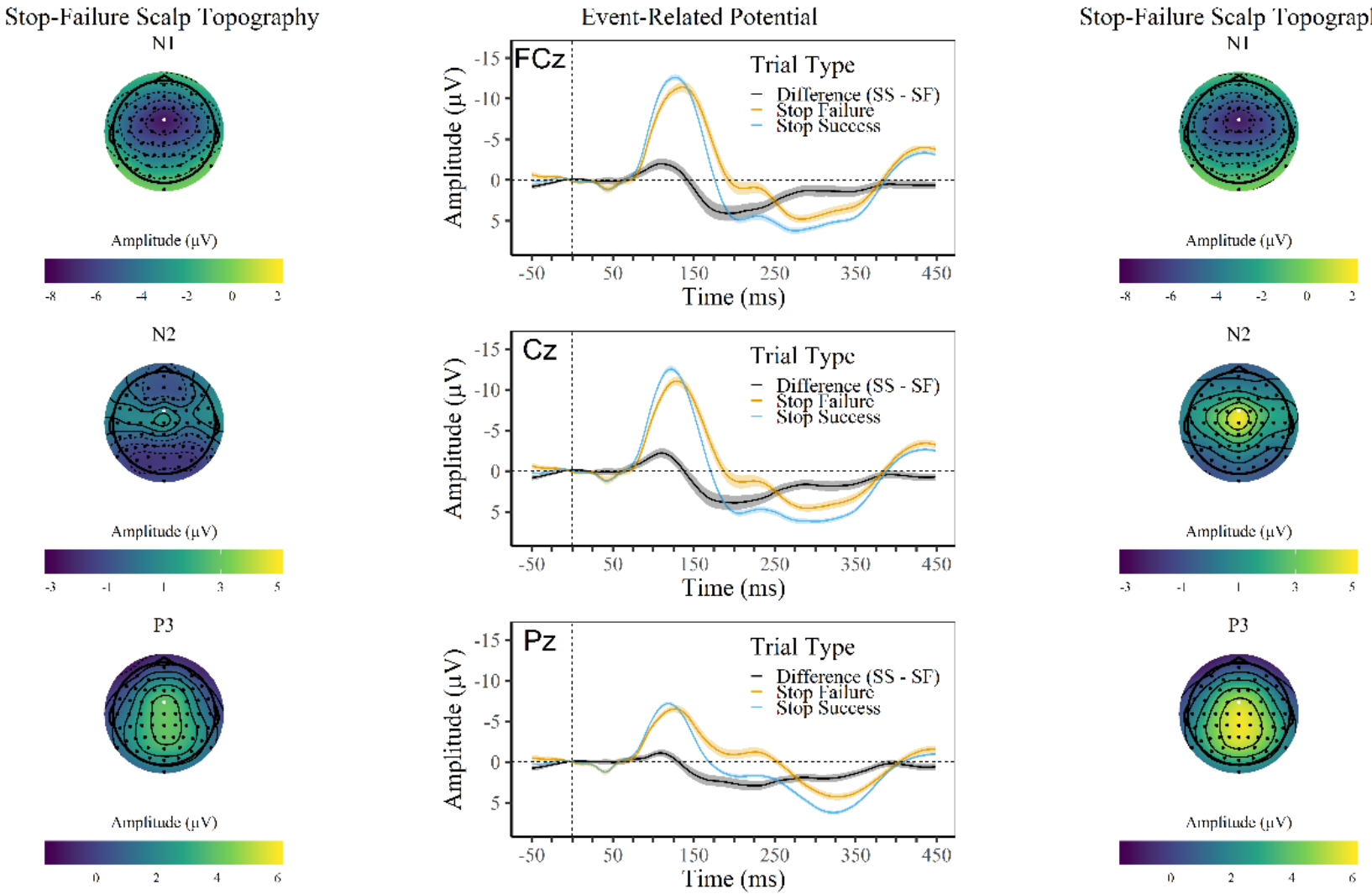


***Figure 2. ERP waveforms for stop-success and stop-failure trials, and their difference are presented at midline fronto-central, central, and parietal sites (middle). The scalp topography for each component measure is presented for stop-success trials (left) and stop-failure trials (right).***

### *3.4. Relationships between Traditional SSRT estimates and ERP measures*

Table 2 provides summary statistics for the Pearson correlation analysis between $SSRT_{int}$ and ERP component measures. Participants with faster $SSRT_{int}$ showed increased N1 amplitude on both trial types (Table 2). However, latency and onset were only found to relate on stop-failure trials. Furthermore, there was weak evidence for a null relationship between N1 onset on stop success trials and $SSRT_{int}$ ($BF_{10}$ = .211). Delayed onset and latency of the stop-failure N1 was found to correlate with faster $SSRT_{int}$. This paradoxical result suggests that participants with later encoding and attention to the stop-signal have faster SSRT.

***Table 2. Pearson product moment correlations and associated Bayes factors for the relationships between event-related potential component measures and $SSRT_{int}$.***

| | | *r* | $BF_{10}$ |
|---|---|---|---|
| **Stop Success** | | | |
| **N1** | | | |
| | *Onset* | .042 | .211 |
| | *Latency* | -.102 | .401 |
| | *Amp* | .405 | $1.08e^{5}$ |
| **N2** | | | |
| | *Amp* | -.311 | 355.522 |
| **P3** | | | |
| | *Onset* | .181 | .916 |
| | *Latency* | .239 | 14.716 |
| | *Amp* | -.347 | $2.55e^{3}$ |

| | | | |
|---|---|---|---|
| **Stop Failure** | | | |
| **N1** | | | |
| | *Onset* | -.266 | 43.028 |
| | *Latency* | -.476 | $3.39e^{7}$ |
| | *Amp* | .350 | $2.95e^{3}$ |
| **N2** | | | |
| | *Amp* | .031 | .2 |
| **P3** | | | |
| | *Onset* | .169 | .898 |
| | *Latency* | .177 | 1.881 |
| | *Amp* | -.388 | $3.39e^{4}$ |

*Note.* Shading indicates at least weak evidence in favour of the correlation. Cross-hatching indicates at least weak evidence in favour of a null correlation.

Mean N2 amplitude showed a negative correlation to $SSRT_{int}$ on stop-success trials, suggesting larger N2 amplitude was related to slower SSRT. Conversely, on stop-failure trials there was weak evidence in favour of a null relationship between N2 mean amplitude and $SSRT_{int}$ ($BF_{10}$ = .2). Consistent with the literature, amplitude of the P3 was negatively correlated with $SSRT_{int}$ on both trial types (Raud & Huster, 2017). Greater P3 amplitude was generated by participants with faster SSRT. Peak latency of the P3 on stop-success trials was also found to correlate with $SSRT_{int}$, suggesting that earlier peaking P3 is associated with reduced SSRT. We were unable to find relationships between P3 onset and $SSRT_{int}$ on either which has also been reported elsewhere (Raud & Huster, 2017; but see Wessel & Aron, 2015), with Bayes factor evidence for the relationships equivocal for both trial types (Table 2).

### *3.5. Plausible Values Relationships*

We first present the results of the plausible values relationships between $SSRT_{int}$ and EXG3 model parameters in text. These are described by their median ρ, Bayesian *p* value, and 95% credible intervals. We then summarise the plausible values relationships between ERP component measures and EXG3 model parameters in Table 3. Small Bayesian *p*-values suggest the distributions are shifted away from zero. The smaller the credible interval, the

more peaked the distribution and the greater the confidence we can have in the median ρ values.

*3.5.1. Relationships between Traditional SSRT estimates and Model Parameters.* We examined the plausible values relationships between $SSRT_{int}$ and key parameters estimated by the EXG3 model (e.g., $SSRT_{EXG3}$, trigger failure, go failure etc.). The two SSRT estimates, $SSRT_{int}$ and $SSRT_{EXG3}$, were moderately related, ρ = .537, $p_{Bayes}$ < .001 [95% CI: .373, .670). In contrast, slower traditional $SSRT_{int}$ was strongly correlated with higher trigger failure rates, ρ = .846, $p_{Bayes}$ < .001 [.787, .89], but only weakly with higher rates of go failure, ρ = .246, $p_{Bayes}$ = .001 [.088, .391]. Importantly, we can show that the plausible values distributions for the relationship between $SSRT_{int}$ and $SSRT_{EXG3}$ is weaker than the relationship between $SSRT_{int}$ and trigger failure. The resulting distribution after taking the difference between the plausible values distributions had a Bayesian *p*-value = .002, showing that only ≈.2% of the difference overlaps zero. In sum, the novel trigger failure parameter was a better predictor of traditional SSRT than the EXG3 estimation of SSRT.

*3.5.2. Relationships between Model Estimated SSRT and ERP measures*. As was found with $SSRT_{int}$, delayed N1 peak latency was related to faster $SSRT_{EXG3}$ on stop-failure trials, ρ = -.362, $p_{Bayes}$ <.001 [-.51, -.19], but not on stop-success trials (Table 3). In addition, larger N1 was associated with faster $SSRT_{EXG3}$ on both stop-failure (ρ = .314, $p_{Bayes}$ <.001 [.15, .46]) and stop-success trials (ρ = .35, $p_{Bayes}$ <.001 [.18, .5]). However, unlike what was found with $SSRT_{int}$, there was no reliable relationship between stop-failure N1 onset and $SSRT_{EXG3}$. In summary, faster $SSRT_{EXG3}$ was associated with larger, but delayed N1 peak, but not with N1 onset latency (Table 3).

Larger stop-success N2 amplitude was associated with slower $SSRT_{EXG3}$, ρ = -.34, $p_{Bayes}$ <.001 [-.49, -.17]. This relationship was also found with $SSRT_{int}$ with a similar correlational strength. Larger P3 amplitude was associated with faster $SSRT_{EXG3}$ across both trial types (Table 3), with both ρ > -.31. For stop-failure trials, later P3 onset and peak latency were both reliably associated with slower $SSRT_{EXG3}$ (Table 3). These relationships were not found with traditional $SSRT_{int}$. In fact, the relationship between P3 onset and $SSRT_{int}$ was found for stop-success trials, not stop-failure trials as was found with $SSRT_{EXG3}$.

Although the strength of the relationship between $SSRT_{EXG3}$ and N1 latency was larger than with P3 latency, this difference was not reliably different from zero ($p_{Bayes}$ = .22).

Likewise, there was no reliable difference between the plausible values distributions of the N1 and P3 amplitude for either trial type ($p_{Bayes}$ >.01). Therefore, we cannot support our prediction that relationships with $SSRT_{EXG3}$ would be stronger with N1, as compared to P3. The plausible value analysis with variance of $SSRT_{EXG3}$ can be found in the supplementary materials. Overall, there was no reliable relationships between the variability of $SSRT_{EXG3}$ and the ERP component measures.

**Table 3. Results of the plausible values analysis. Median ρ, Bayesian p-values, and 95% credible intervals for the relationship between model estimated response inhibition parameters and event-related potential component measures.**

| | | Stop Signal Reaction Time | | | Probability of Trigger Failure | | | Probability of Go Failure | | | Matching Go Finishing Time | | |
|---|---|---|---|---|---|---|---|---|---|---|---|---|---|
| | | ρ | $p_{Bayes}$ | CI | ρ | $p_{Bayes}$ | CI | ρ | $p_{Bayes}$ | CI | ρ | $p_{Bayes}$ | CI |
| **Stop Success** | | | | | | | | | | | | | |
| **N1** | *Onset* | 0 | .501 | [-.18, .18] | .055 | .255 | [-.11, .22] | .165 | .021 | [.01, .32] | .141 | .04 | [-.02, .29] |
| | *Latency* | -.09 | .174 | [-.26, .09] | -.07 | .219 | [-.23, .1] | .014 | .432 | [-.15, .17] | .137 | .044 | [-.02, .29] |
| | *Amp* | .35 | <.001 | [.18, .5] | .289 | <.001 | [.13, .43] | -.064 | .234 | [-.22, .1] | -.149 | .036 | [-.3, .01] |
| **N2** | | | | | | | | | | | | | |
| | *Amp* | -.34 | <.001 | [-.49, -.17] | -.182 | .016 | [-.34, -.02] | .081 | .16 | [-.08, .24] | .333 | <.001 | [.19, .47] |
| **P3** | | | | | | | | | | | | | |
| | *Onset* | .186 | .065 | [-.06, .41] | .076 | .249 | [-.14, .29] | .089 | .208 | [-.13, .3] | .123 | .127 | [-.09, .32] |
| | *Latency* | .194 | .014 | [.02, .36] | .127 | .064 | [-.04, .28] | .021 | .401 | [-.14, .18] | .029 | .361 | [-.13, .18] |
| | *Amp* | -.342 | <.001 | [-.49, -.18] | -.207 | .007 | [-.36, -.05] | -.076 | .192 | [-.23, .08] | .117 | .073 | [-.04, .27] |
| **Stop Failure** | | | | | | | | | | | | | |
| **N1** | *Onset* | -.145 | .06 | [-.31, .03] | -.257 | .001 | [-.4, -.1] | .013 | .436 | [-.15, .17] | .211 | .004 | [.06, .36] |
| | *Latency* | -.362 | <.001 | [-.51, -.19] | -.412 | <.001 | [-.54, -.26] | -.097 | .129 | [-.25, .06] | .263 | .001 | [.11, .4] |
| | *Amp* | .314 | <.001 | [.15, .46] | .206 | .006 | [.05, .36] | -.119 | .082 | [-.27, .04] | -.156 | .03 | [-.31, 0] |
| **N2** | | | | | | | | | | | | | |
| | *Amp* | -.095 | .166 | [-.27, .09] | .106 | .102 | [-.06, .26] | .132 | .052 | [-.03, .29] | .202 | .006 | [.05, .35] |
| **P3** | | | | | | | | | | | | | |
| | *Onset* | .26 | .01 | [.04, .45] | .067 | .257 | [-.14, .26] | .083 | .206 | [-.12, .27] | -.037 | .374 | [-.23, .16] |
| | *Latency* | .249 | .003 | [.07, .41] | .069 | .208 | [-.1, .23] | -.019 | .433 | [-.18, .14] | -.081 | .173 | [-.24, .08] |
| | *Amp* | -.313 | <.001 | [-.47, -.14] | -.279 | .001 | [-.42, -.12] | -.048 | .3 | [-.21, .11] | .139 | .041 | [-.02, .29] |

*Note.* ρ = Median of the posterior distribution of the population correlation. $p_{Bayes}$ = Bayesian *p* value. CI = Credible Interval [2.5%, 97.5%]. Shading indicates reliable relationships (i.e., $p_{Bayes}$ <.01).

*3.5.3. ERP Relationships with Probability of Trigger Failure*. As shown in Table 3, for stop-failure trials only, earlier N1 peak latency, and to a lesser degree, N1 onset latency, were associated with higher rates of trigger failure. This N1 peak latency effect replicates the finding by Matzke, Hughes et al. (2017), but extends it to show specificity to stop-failure trials and to also include N1 onset latency. In addition, larger N1 peak amplitude for both trial types was associated with lower rate of trigger failure. As expected, lower levels of attention to the stop signal (i.e., reduced N1 amplitude) was related to higher rates of trigger failure. Rate of trigger failure was not associated with N2 mean amplitude, and P3 onset or peak latency for either trial type (Table 3). However, for both trial types, P3 peak amplitude was smaller for participants with higher rates of trigger failure (average ρ ≈ -.25; Table 3).

*3.5.4. ERP relationships with Finishing Time of the Matching Go Runner.* Later N1 onset and peak latency on stop-failure trials were correlated with slower go finishing time (ρ ≈ .23). For both trial types, larger N2 amplitude was correlated with faster matching go finishing times (Table 3).

### *3.6. N1 Peak Latency and Trigger Failure Rate*

We ran further exploratory analyses to understand the paradoxical finding that faster N1 latency on stop-failure trials is associated with higher rates of trigger failure. Figure 1.B shows that the distribution of trigger failure has a strong right skew that spreads out past ≈20%. We examined whether there are differences in the pattern of ERP effects as a function on trigger failure rate by extracting ERP waveforms for three groups of participants based on a tertile split of median participant-level posterior trigger failure rates: Low (<14%), Mid (>= 14% and =<25.8%) and High (>25.8%), n=52 per group. The groups had similar age (Low = 20.4; Mid = 21.5; High = 20.65) and gender distribution (Low = 48.1% Female; Mid = 53.8% Female; High = 57.7% Female).

ERPs for each group are compared in Figure 3, and summary statistics for N1 peak latency are shown in Table 4. A Bayesian mixed ANOVA using default JASP priors (JASP Team, 2018) of N1 peak latency at FCz with trigger failure group (High, Mid, Low) and trial type (stop-failure, stop-success) as factors showed that the evidence for the model containing the two main effects was very strong ($BF_{10} = 6.43e^{16}$). The interaction model was also supported when controlling for the main effects of group and trial type ($BF_{Inclusion} = 1.1e^{9}$). Both Low and Mid trigger failure groups show a large N1 that peaked earlier for stop-success than

stop-failure trials, whereas N1 did not differ by trial type in the High trigger failure group (Table 4).

**Table 4. Summary of the N1 peak latency difference between Low, Mid, and High trigger failure groups.**

| Group | Stop Success (SD) | Stop Failure (SD) | Trial Difference ($BF_{10}$) | Effect Size (δ) |
|---|---|---|---|---|
| **Low** | 129.6 (9.7) | 139.7 (10.36) | $4.85e^{13}$ | -1.632 |
| **Mid** | 128.13 (7.8) | 133.37 (8.67) | $1.34e^{6}$ | -.918 |
| **High** | 125.9 (9.1) | 126.6 (9.23) | .2 | -.103 |

*Note.* Effect sizes are for the success – failure trial type difference. Shading indicates at least weak evidence in favour of the trial type difference. Cross-hatching indicates at least weak evidence in favour of a null difference.

Furthermore, there was an interesting pattern of differences in N1 peak latency across trigger failure groups. The Low and Mid trigger failure groups did not differ in N1 peak latency on stop-success trials, $BF_{10}$ = .283, δ = .15, but N1 peaked earlier on stop-failure trials in the Mid trigger failure group ($BF_{10}$ = 29.39, δ = .61). Comparing Low and High trigger failure groups also showed strong evidence in favour of an earlier N1 peak latency for stop-failure trials in the High trigger failure group, $BF_{10} = 1.26e^{7}$, δ = 1.28, but the evidence for the same difference on stop-success trials was equivocal, $BF_{10}$ = 1.24, δ = .36. The same results were found when comparing the Mid to High trigger failure groups: stop-failure, $BF_{10}$ = 117.61, δ = .7; stop-success, $BF_{10}$ = .47, δ = .24.

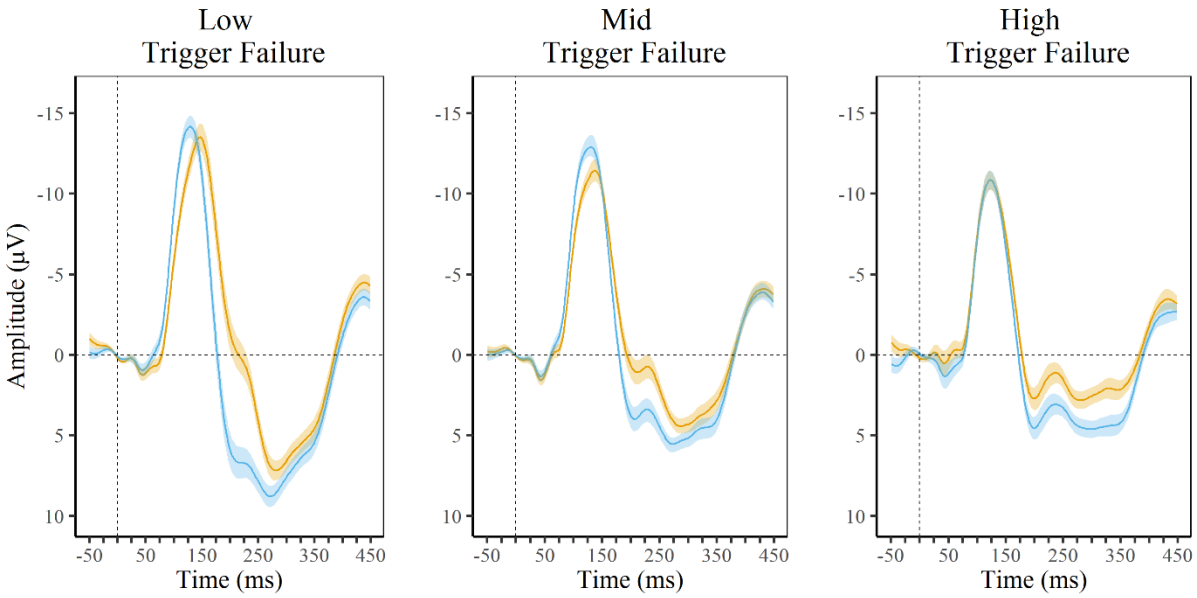


**Figure 3. ERPs for stop-success (blue) and stop-failure (orange) shown for low, mid and high trigger failure groups at FCz. Shaded areas represent the within subject confidence intervals.**

## 4. Discussion

This study is the first to make a comprehensive examination of the ERP correlates of response inhibition using an ex-Gaussian model of response inhibition which accounts for the failures of both the stop and go processes. These relationships suggested a number of interpretive changes to common ERP components found during the stop-signal task. We present the evidence and interpretations for each of the ERP components separately, but first compare the model-based estimates of SSRT with traditional non-parametric estimates that have been recently been recommended as best practice (Verbruggen et al., 2019).

### *4.1. Integration vs ex-Gaussian estimates of SSRT*

Replicating recent studies, we show that ex-Gaussian estimation techniques which account for trigger failure result in substantial attenuation of SSRT latency. $SSRT_{EXG3}$ was about 65ms faster compared to SSRT using the traditional integration algorithm (Matzke, Curley, et al., 2019; Matzke, Hughes, et al., 2017; Skippen et al., 2019; Weigard et al., 2019). These findings support the proposal that traditional SSRT estimates are biased by the assumption that trigger failure rates are negligible. Importantly, the traditionally estimated $SSRT_{int}$ was only moderately correlated with ex-Gaussian model estimated $SSRT_{EXG3}$ and more strongly associated with the trigger failure parameter. This suggests that previous interpretations, based on a non-parametric SSRT, of ERP components in terms of the latency of an inhibitory response may be spurious and instead these components are more likely

related to a failure to engage the correct task goal (i.e., failure to trigger a stop response).

### *4.2. Attention, N1, and Response Inhibition*

We first discuss the 'stop-N1' effects which have been relatively unexplored compared to other ERP components in studies using the stop-signal task. In this study, we support the general finding that N1 amplitude is larger on stop-success compared to stop-failure trials. We also report a moderate positive relationship between SSRT and N1 amplitude, which is found for both trial types and both the traditional and ex-Gaussian estimations of SSRT. This relationship supports Keneman's (2015) interpretation of the 'stop-N1' effect. Larger N1 amplitude on stop-success compared to stop-failure trials is thought to indicate greater attentional allocation to the stop signal, which in turn influences the outcome of a stop trial (Bekker et al., 2005; Hughes et al., 2012; Kenemans, 2015; but see Ramautar, Slagter, Kok, & Ridderinkhof 2006). If fluctuations in attention influence both N1 amplitude and the outcome of a stop trial, then our evidence suggests that this 'stop-N1' effect is elicited through the relationship between reduced SSRT and increased N1 amplitude. This study is the first to show that individual variability in attentional allocation to the task can change SSRT, which in turn modulates the probability of successful inhibition.

Furthermore, we present the first evidence that a 'stop-N1' effect is also present for the N1 component's latency. We found that not only does successful stopping depend on the amplitude of the N1, but also its latency. As the N1 starts earlier, peaks earlier, and is larger on stop-success trials when compared to stop-failure trials, it appears to index a cognitive process which determines the success of inhibition. Importantly, this effect was only seen in participants with low to mid range levels of trigger failure. Those participants with high levels of trigger failure (>25%) did not show a difference in latency between trial types.

Traditionally, the very early time-course (within 200ms after the stop signal), especially compared to the traditional estimates of SSRT, N1 has been discounted from any direct role in the inhibition process. However, recent support for a fast, automatic inhibitory process (e.g., Verbruggen, McLaren, & Chambers, 2014) suggests that the N1 may in fact be a better temporal index of the stop process than N2 or P3. These findings are consistent with the argument that the manifestation of the inhibitory process, which has previously been attributed to the P3, may in fact be better represented by the N1, an earlier ERP component associated with attention to the stimulus. As stop-failure N1 peak latency was related to

both traditional and ex-Gaussian estimates of SSRT, we propose that N1 peak latency may indicate the starting point of the inhibitory process. In fact, the ex-Gaussian estimates of SSRT temporally match that of the N1 peak latency (both ≈130ms). However, this finding requires replication to suggest such a connection with strong confidence.

Nevertheless, the attentionally sensitive N1 component appears to be imperative to successful inhibition through the detection and encoding of the stop signal. Dysfunctional attentional processing of the stop signal has previously been suggested to lead to a seemingly earlier peaking N1 for participants with larger rates of trigger failure in a schizophrenia patient group (Matzke, Hughes, et al., 2017). We provide evidence in line with this finding in a large healthy cohort, and also extend this to show that it is only present on stop-failure trials. However, the fact that N1 onset was also found to correlate with trigger failure (albeit to a lesser degree) suggests that the effect might not be specifically related to the dysfunction of later sub-components of the N1 as previously thought (Matzke, Hughes, et al., 2017). The ERP morphology of the high and low trigger failure groups in Figure 3 suggests that the phenomenon of trigger failure is closely tied to the attentional allocation to the stop signal more generally.

The absence of a 'stop-N1' effect in the high trigger failure group suggests a broken connection between the impact of the stop signal and the outcome of the trial. Therefore, the paradoxical correlation between earlier peaking latency of the N1 and higher rates of trigger failure can be explained by an overall earlier stop-failure N1 in the high trigger failure group. Based on the evidence presented here, this might then reflect the lack of connection, which is proposed to be represented by tonic activity in the right inferior frontal gyrus (rIFG; Kenemans, 2015). Specifically, Kenemans proposed that a tonically active rIFG potentiates the link between detecting the stop signal and eliciting an inhibitory process. When this link is active, stopping is speeded and possibly automatic (Verbruggen, Best, et al., 2014). The ≈130ms estimates of SSRT reported here (see also, Skippen et al., 2019) supports the idea that inhibition can be automatic and adds to a growing literature reporting similar evidence in the form of short SSRT latencies (Matzke, Hughes, et al., 2017) and physiological evidence of fast inhibitory processes around 140ms (Coxon, Stinear, & Byblow, 2006; Raud & Huster, 2017; Waldvogel et al., 2000; Wilcoxon, Nadolski, Samarut, Chassande, & Redei, 2007). We suggest that in line with Kenemans (2015) explanation for the absence of a 'stop-N1' in patients with attention deficit hyperactivity disorder, there is a missing automatic connection between the registration of the stop signal (as represented by the N1) and the

outcome of the trial (i.e., failed or successful inhibition) in participants with high trigger failure rates. Recent analysis strengthens this argument by showing that increased rates of trigger failure drove group differences between children with attention deficit hyperactivity disorder and typically developing controls. Poor SST performance among children with attention deficit hyperactivity disorder likely reflects impairments in early attentional processes, rather than the speed of the stop process (Weigard, et al., 2019).

Further investigation is warranted, but we suggest that this gating mechanism proposed to reflect rIFG activation, marked by a beta signature around the time of $SSRT_{EXG3}$ is rudimentarily captured in our N1. The N1 reported here shows similar trial type differences, scalp topography, and timing as a beta frequency response which occurs before traditional estimates of SSRT (i.e., ≈150ms after the stop signal) and appears to be imperative for successful stopping (Huster, Schneider, Lavallee, Enriquez-Geppert, & Herrmann, 2017; Swann et al., 2009; Swann et al., 2012; Wagner, Wessel, Ghahremani, & Aron, 2018; Wessel, Conner, Aron, & Tandon, 2013). This beta signature shows much of the same trial type characteristics as both the N1 and P3 ERP components, but temporally aligns with the N1. More generally, we provide evidence that shows that ERP attributes previously related to the speed of the inhibitory response (i.e., SSRT) are more related to attentional processes that occur much earlier.

**4.3. Conflict and Control N2**

Correlations showing larger N2 amplitude on stop-failure trials in participants with slower SSRT has been previously reported (van Boxtel, van der Molen, Jennings, & Brunia, 2001). However, the explanation that this then reflects the manifestation of the inhibitory process is not supported here. Firstly, we found evidence in favour of a null relationship between stop-failure N2 amplitude and $SSRT_{int}$. Secondly, both the $SSRT_{int}$ and $SSRT_{EXG3}$ estimates do not coincide with the N2 component. We instead believe our relationships between stop-success N2 and SSRT, coupled with the fact that we report larger N2 amplitude on stop-failure trials to reflect the conflict stop-N2 hypothesis.

A general interpretation for the increased stop-N2 amplitude on stop-failure trials (Dimoska, Johnstone, & Barry, 2006; Galdo-Alvarez, Bonilla, González-Villar, & Carrillo-de-la-Peña, 2016; Greenhouse & Wessel, 2013; Ramautar, Kok, & Ridderinkhof, 2006; van Boxtel et al., 2001) is that it indexes the increased level of conflict that occurs when the go and stop process are both maximal (Ramautar et al., 2004; Ramautar, Kok, et al., 2006). In our data, larger stop-success N2 was related with slower SSRT, and larger N2 for both trial types was

associated with faster finishing time of the matching go process. Our N2 is larger on stop-failure trials, where the go process is likely to be relatively faster, and the stop process relatively slower, leading both processes to be maximally active at the same time. Therefore, there is greater conflict on stop-failure trials, which may be captured in the N2.

### *4.4. Manifestation of Response Inhibition and the P3*

The $SSRT_{int}$ estimate was almost 100ms earlier than P3 onset latency at the group level and there was no relationship found between P3 onset and $SSRT_{int}$. Furthermore, we only found weak support for the relationship between stop-success P3 latency and $SSRT_{int}$. This does not support the P3 as an electrophysiological manifestation of the stop process (Wessel & Aron, 2015). In contrast, $SSRT_{EXG3}$ which was, on average, 140ms earlier than the onset latency of the P3, was reliably correlated with both P3 onset and peak latency on stop-failure trials. Given that $SSRT_{EXG3}$ also correlated with N1 peak latency on stop-failure trials, we suggest that the P3 on stop-failure trials may represent the activation of an evaluation process after a failure to inhibit, a process which, by definition, would be elicited only after the inhibition process has failed.

Alternatively, recent work has shown that the P3 on the stop-signal task shares common neural generators with the P3 elicited in tasks involving infrequent stimulus detection (Waller, Hazeltine, & Wessel, 2019; Wessel & Huber, 2019). If P3 indexes a stimulus detection process, the larger P3 on stop-success compared to stop-failure trials might simply index the successful detection of the stop signal on the former and/or poor detection on the later trial type. This interpretation is consistent with both the horse-race model in general, as well as the interpretations of the N1 findings presented here. Specifically, we propose that P3 is not a manifestation of the stopping process itself, but a delayed marker of detection of the stop signal. Therefore, the attentional processes required to both detect the novelty of the stop signal, as well as trigger an inhibitory response, may help explain the relationship between trigger failure and P3 amplitude across trial types.

**Acknowledgements**

We thank Gavin Cooper for paradigm programming and all members of the Age-ility Project past and present for assistance with data collection/entry. Special thanks to Montana McKewen and Patrick Cooper for their contributions to project management. We would also like to thank participants for their time.

**Funding Sources**

This research was supported by an Australian Research Council Discovery Project (DP120100340, DP170100756) to FK and PM. PS was supported by a Research Training Program Stipend. DM is supported by a Veni grant (451-15-010) from the Netherlands Organization of Scientific Research (NWO).

## References

Band, G., Van Der Molen, M., & Logan, G. (2003). Horse-race model simulations of the stop-signal procedure. *Acta Psychologica, 112*(2), 105-142.

Bari, A., & Robbins, T. W. (2013). Inhibition and impulsivity: behavioral and neural basis of response control. *Progress in neurobiology, 108*, 44-79.

Bekker, E. M., Kenemans, J., Hoeksma, M. R., Talsma, D., & Verbaten, M. N. (2005). The pure electrophysiology of stopping. *International Journal of Psychophysiology, 55*(2), 191-198. doi:http://dx.doi.org/10.1016/j.ijpsycho.2004.07.005

Chatham, C. H., Claus, E. D., Kim, A., Curran, T., Banich, M. T., & Munakata, Y. (2012). Cognitive Control Reflects Context Monitoring, Not Motoric Stopping, in Response Inhibition. *PLoS ONE, 7*(2), e31546. doi:10.1371/journal.pone.0031546

Cooper, P. S., Wong, A. S., Fulham, W. R., Thienel, R., Mansfield, E., Michie, P. T., & Karayanidis, F. (2015). Theta frontoparietal connectivity associated with proactive and reactive cognitive control processes. *NeuroImage, 108*, 354-363.

Coxon, J. P., Stinear, C. M., & Byblow, W. D. (2006). Intracortical Inhibition During Volitional Inhibition of Prepared Action. *J Neurophysiol, 95*, 3371-3383.

Dimoska, A., & Johnstone, S. J. (2008). Effects of varying stop-signal probability on ERPs in the stop-signal task: do they reflect variations in inhibitory processing or simply novelty effects? *Biological Psychology, 77*(3), 324-336.

Dimoska, A., Johnstone, S. J., & Barry, R. J. (2006). The auditory-evoked N2 and P3 components in the stop-signal task: indices of inhibition, response-conflict or error-detection? *Brain and Cognition, 62*(2), 98-112.

Falkenstein, M., Hoormann, J., & Hohnsbein, J. (1999). ERP components in Go/Nogo tasks and their relation to inhibition. *Acta Psychologica, 101*(2), 267-291.

Fulham, W., R. (2015). EEGDisplay v6.4.4 [Software]. *Available from the author: University of Newcastle, NSW, Australia*.

Galdo-Alvarez, S., Bonilla, F. M., González-Villar, A. J., & Carrillo-de-la-Peña, M. T. (2016). Functional Equivalence of Imagined vs. Real Performance of an Inhibitory Task: An EEG/ERP Study. *Frontiers in Human Neuroscience, 10*, 467. doi:10.3389/fnhum.2016.00467

Gelman, A., & Rubin, D. B. (1992). Inference from iterative simulation using multiple sequences. *Statistical science, 7*(4), 457-472.

González-Villar, A. J., Bonilla, F. M., & Carrillo-de-la-Peña, M. T. (2016). When the brain simulates stopping: Neural activity recorded during real and imagined stop-signal tasks. *Cognitive, Affective, & Behavioral Neuroscience, 16*(5), 825-835. doi:10.3758/s13415-016-0434-3

Greenhouse, I., & Wessel, J. R. (2013). EEG signatures associated with stopping are sensitive to preparation. *Psychophysiology, 50*(9), 900-908.

Heathcote, A., Lin, Y.-S., Reynolds, A., Strickland, L., Gretton, M., & Matzke, D. (2018). Dynamic models of choice. *Behavior Research Methods*. doi:10.3758/s13428-018-1067-y

Hillyard, S. A., Hink, R. F., Schwent, V. L., & Picton, T. W. (1971). Electrical Signs of Selective Attention in the Human Brain. *Conditional Reflex, 6*, 215.

Hughes, M., Fulham, W. R., Johnston, P. J., & Michie, P. T. (2012). Stop-signal response inhibition in schizophrenia: Behavioural, event-related potential and functional neuroimaging data. *Biological Psychology, 89*, 220-231.

Huster, R. J., Enriquez-Geppert, S., Lavallee, C. F., Falkenstein, M., & Herrmann, C. S. (2013). Electroencephalography of response inhibition tasks: functional networks and cognitive contributions. *International Journal of Psychophysiology, 87*(3), 217-233.

Huster, R. J., Schneider, S., Lavallee, C. F., Enriquez-Geppert, S., & Herrmann, C. S. (2017). Filling the void-enriching the feature space of successful stopping. *Hum Brain Mapp, 38*(3), 1333-1346. doi:10.1002/hbm.23457

JASP Team. (2018). JASP (Version 0.9).

Karayanidis, F., Keuken, M. C., Wong, A., Rennie, J. L., de Hollander, G., Cooper, P. S., . . . Phillips, N. (2016). The Age-ility Project (Phase 1): Structural and functional imaging and electrophysiological data repository. *Neuroimage, 124*, 1137-1142.

Kass, R. E., & Raftery, A. E. (1995). Bayes factors. *Journal of the american statistical association, 90*(430), 773-795.

Kenemans, J. L. (2015). Specific proactive and generic reactive inhibition. *Neurosci Biobehav Rev, 56*, 115-126. doi:10.1016/j.neubiorev.2015.06.011

Kiesel, A., Miller, J., Jolicœur, P., & Brisson, B. (2008). Measurement of ERP latency differences: A comparison of single-participant and jackknife-based scoring methods. *Psychophysiology, 45*(2), 250-274.

Kok, A., Ramautar, J. R., De Ruiter, M. B., Band, G. P., & Ridderinkhof, K. R. (2004). ERP components associated with successful and unsuccessful stopping in a stop-signal task. *Psychophysiology, 41*(1), 9-20.

Lansbergen, M. M., Böcker, K. B., Bekker, E. M., & Kenemans, J. L. (2007). Neural correlates of stopping and self-reported impulsivity. *Clinical Neurophysiology, 118*(9), 2089-2103.

Lipszyc, J., & Schachar, R. (2010). Inhibitory control and psychopathology: a meta-analysis of studies using the stop signal task. *Journal of the International Neuropsychological Society, 16*(06), 1064-1076.

Logan, G. D. (1994). On the ability to inhibit thought and action: A users' guide to the stop signal paradigm.

Logan, G. D., & Cowan, W. B. (1984). On the ability to inhibit thought and action: A theory of an act of control. *Psychological Review, 91*(3), 295.

Lopez-Calderon, J., & Luck, S. J. (2014). ERPLAB: an open-source toolbox for the analysis of event-related potentials. *Frontiers in Human Neuroscience, 8*, 213.

Luck, S. J., Woodman, G. F., & Vogel, E. K. (2000). Event-related potential studies of attention. *Trends in Cognitive Sciences, 4*(11), 432-440.

Ly, A., Boehm, U., Heathcote, A., Turner, B., Forstmann, B., Marsman, M., . . . Moustafa, A. (2018). A flexible and efficient hierarchical Bayesian approach to the exploration of individual differences in cognitive-model-based neuroscience. *Computational Models of Brain and Behavior*, 467-480.

Mathworks. (r2018b). MATLAB.

Matzke, D., Curley, S., Gong, C. Q., & Heathcote, A. (2019). Inhibiting responses to difficult choices. *Journal of Experimental Psychology: General, 148*(1), 124.

Matzke, D., Dolan, C. V., Logan, G. D., Brown, S. D., & Wagenmakers, E.-J. (2013). Bayesian parametric estimation of stop-signal reaction time distributions. *Journal of Experimental Psychology: General, 142*(4), 1047.

Matzke, D., Hughes, M., Badcock, J. C., Michie, P., & Heathcote, A. (2017). Failures of cognitive control or attention? The case of stop-signal deficits in schizophrenia. *Atten Percept Psychophys, 79*(4), 1078-1086. doi:10.3758/s13414-017-1287-8

Matzke, D., Love, J., & Heathcote, A. (2016). A Bayesian approach for estimating the probability of trigger failures in the stop-signal paradigm. *Behavior research methods*, 1-15.

Matzke, D., Love, J., & Heathcote, A. (2017). A Bayesian approach for estimating the probability of trigger failures in the stop-signal paradigm. *Behavior Research Methods, 49*(1), 267-281. doi:10.3758/s13428-015-0695-8

Matzke, D., Love, J., Wiecki, T. V., Brown, S. D., Logan, G. D., & Wagenmakers, E.-J. (2013). Release the BEESTS: Bayesian ex-Gaussian estimation of stop-signal reaction time distributions. *Frontiers in Psychology: Quantitative Psychology and Measurement, 4*. doi:10.3389/fpsyg.2013.00918

Matzke, D., Verbruggen, F., & Logan, G. D. (2019). The stop-signal paradigm. In E. J. Wagenmakers (Ed.), *Stevens' Handbook of Experimental Psychology and Cognitive Neuroscience* (Vol. 5): John Wiley & Sons.

Morey, R., & Rouder, J. (2018). BayesFactor: Computation of Bayes Factors for Common Designs (Version 0.9.12-4.2). Retrieved from https://CRAN.R-project.org/package=BayesFactor

Morey, R. D. (2008). Confidence Intervals from Normalized Data: A correction to Cousineau (2005). *Tutorials in Quantitative Methods for Psychology, 4*, 61-64.

Näätänen, R. (1982). Processing negativity: An evoked-potential reflection. *Psychological Bulletin, 92*(3), 605.

Näätänen, R., Gaillard, A. W., & Mäntysalo, S. (1978). Early selective-attention effect on evoked potential reinterpreted. *Acta Psychologica, 42*(4), 313-329.

Näätänen, R., & Michie, P. T. (1979). Early selective-attention effects on the evoked potential: a critical review and reinterpretation. *Biological Psychology, 8*(2), 81-136.

Näätänen, R., & Picton, T. (1987). The N1 wave of the human electric and magnetic response to sound: a review and an analysis of the component structure. *Psychophysiology, 24*(4), 375-425.

Pires, L., Leitão, J., Guerrini, C., & Simões, M. R. (2014). Event-related brain potentials in the study of inhibition: cognitive control, source localization and age-related modulations. *Neuropsychology review, 24*(4), 461-490.

R Core Team. (2018). R: A language and environment for statistical computing. Vienna, Austria: R Foundation for Statistical Computing. Retrieved from https://www.R-project.org/

Ramautar, J. R., Kok, A., & Ridderinkhof, K. R. (2004). Effects of stop-signal probability in the stop-signal paradigm: The N2/P3 complex further validated. *Brain and Cognition, 56*(2), 234-252. doi:http://dx.doi.org/10.1016/j.bandc.2004.07.002

Ramautar, J. R., Kok, A., & Ridderinkhof, K. R. (2006). Effects of stop-signal modality on the N2/P3 complex elicited in the stop-signal paradigm. *Biological Psychology, 72*(1), 96-109.

Ramautar, J. R., Slagter, H. A., Kok, A., & Ridderinkhof, K. R. (2006). Probability effects in the stop-signal paradigm: The insula and the significance of failed inhibition. *Brain Research, 1105*(1), 143-154. doi:http://dx.doi.org/10.1016/j.brainres.2006.02.091

Raud, L., & Huster, R. J. (2017). The Temporal Dynamics of Response Inhibition and their Modulation by Cognitive Control. *Brain Topography, 30*(4), 486-501. doi:10.1007/s10548-017-0566-y

Sebastian, A., Forstmann, B. U., & Matzke, D. (2018). Towards a model-based cognitive neuroscience of stopping–a neuroimaging perspective. *Neuroscience & Biobehavioral Reviews*.

Semlitsch, H. V., Anderer, P., Schuster, P., & Presslich, O. (1986). A solution for reliable and valid reduction of ocular artifacts, applied to the P300 ERP. *Psychophysiology, 23*(6), 695-703.

Sharma, L., Markon, K. E., & Clark, L. A. (2014). Toward a theory of distinct types of "impulsive" behaviors: A meta-analysis of self-report and behavioral measures. *Psychological Bulletin, 140*(2), 374.

Skippen, P., Matzke, D., Heathcote, A., Fulham, W. R., Michie, P., & Karayanidis, F. (2019). Reliability of triggering inhibitory process is a better predictor of impulsivity than SSRT. *Acta Psychologica, 192*, 104-117.

Spiegelhalter, D. J., Best, N. G., Carlin, B. P., & Van Der Linde, A. (2002). Bayesian measures of model complexity and fit. *Journal of the Royal Statistical Society: Series B (Statistical Methodology), 64*(4), 583-639.

Swann, N., Tandon, N., Canolty, R., Ellmore, T. M., McEvoy, L. K., Dreyer, S., . . . Aron, A. R. (2009). Intracranial EEG reveals a time- and frequency-specific role for the right inferior frontal gyrus and primary motor cortex in stopping initiated responses. *J Neurosci, 29*(40), 12675-12685. doi:10.1523/jneurosci.3359-09.2009

Swann, N. C., Cai, W., Conner, C. R., Pieters, T. A., Claffey, M. P., George, J. S., . . . Tandon, N. (2012). Roles for the pre-supplementary motor area and the right inferior frontal gyrus in stopping action: Electrophysiological responses and functional and structural connectivity. *NeuroImage, 59*(3), 2860-2870. doi:https://doi.org/10.1016/j.neuroimage.2011.09.049

Tannock, R., Schachar, R. J., Carr, R. P., Chajczyk, D., & Logan, G. D. (1989). Effects of methylphenidate on inhibitory control in hyperactive children. *Journal of Abnormal Child Psychology, 17*(5), 473-491.

Ter Braak, C. J. (2006). A Markov Chain Monte Carlo version of the genetic algorithm Differential Evolution: easy Bayesian computing for real parameter spaces. *Statistics and Computing, 16*(3), 239-249.

van Boxtel, G. J., van der Molen, M. W., Jennings, J. R., & Brunia, C. H. (2001). A psychophysiological analysis of inhibitory motor control in the stop-signal paradigm. *Biological Psychology, 58*(3), 229-262.

Verbruggen, F., Aron, A. R., Band, G. P. H., Beste, C., Bissett, P. G., Brockett, A. T., . . . Boehler, C. N. (2019). A consensus guide to capturing the ability to inhibit actions and impulsive behaviors in the stop-signal task. *eLife, 8*, e46323. doi:10.7554/eLife.46323

Verbruggen, F., Best, M., Bowditch, W. A., Stevens, T., & McLaren, I. P. L. (2014). The inhibitory control reflex. *Neuropsychologia, 65*, 263-278. doi:http://dx.doi.org/10.1016/j.neuropsychologia.2014.08.014

Verbruggen, F., & Logan, G. (2009). Models of response inhibition in the stop-signal and stop-change paradigms. *Neuroscience & Biobehavioral Reviews, 33*(5), 647-661.

Verbruggen, F., McLaren, I. P. L., & Chambers, C. D. (2014). Banishing the Control Homunculi in Studies of Action Control and Behavior Change. *Perspectives on Psychological Science, 9*(5), 497-524. doi:10.1177/1745691614526414

Wagner, J., Wessel, J. R., Ghahremani, A., & Aron, A. R. (2018). Establishing a Right Frontal Beta Signature for Stopping Action in Scalp EEG: Implications for Testing Inhibitory Control in Other Task Contexts. *Journal of Cognitive Neuroscience, 30*(1), 107-118. doi:10.1162/jocn_a_01183

Waldvogel, D., van Gelderen, P., Muellbacher, W., Ziemann, U., Immisch, I., & Hallett, M. (2000). The relative metabolic demand of inhibition and excitation. *Nature, 406*(6799), 995.

Waller, D. A., Hazeltine, E., & Wessel, J. R. (2019). Common neural processes during action-stopping and infrequent stimulus detection: The frontocentral P3 as an index of generic motor inhibition. *International Journal of Psychophysiology*. doi:https://doi.org/10.1016/j.ijpsycho.2019.01.004

Weigard, A., Heathcote, A., Matzke, D., & Huang-Pollock, C. (2019). Cognitive Modeling Suggests That Attentional Failures Drive Longer Stop-Signal Reaction Time Estimates in Attention Deficit/Hyperactivity Disorder. *Clinical Psychological Science*. doi:10.1177/2167702619838466

Wessel, J. R., & Aron, A. R. (2015). It's not too late: The onset of the frontocentral P3 indexes successful response inhibition in the stop-signal paradigm. *Psychophysiology, 52*(4), 472-480. doi:10.1111/psyp.12374

Wessel, J. R., Conner, C. R., Aron, A. R., & Tandon, N. (2013). Chronometric electrical stimulation of right inferior frontal cortex increases motor braking. *J Neurosci, 33*(50), 19611-19619. doi:10.1523/JNEUROSCI.3468-13.2013

Wessel, J. R., & Huber, D. E. (2019). Frontal cortex tracks surprise separately for different sensory modalities but engages a common inhibitory control mechanism. *bioRxiv*, 572081. doi:10.1101/572081

Wilcoxon, J. S., Nadolski, G. J., Samarut, J., Chassande, O., & Redei, E. E. (2007). Behavioral inhibition and impaired spatial learning and memory in hypothyroid mice lacking thyroid hormone receptor alpha. *Behavioural Brain Research, 177*(1), 109-116. doi:http://dx.doi.org/10.1016/j.bbr.2006.10.030

Woldorff, M. G. (1993). Distortion of ERP averages due to overlap from temporally adjacent ERPs: analysis and correction. *Psychophysiology, 30*(1), 98-119.